

## **ROBUSTNESS OF SEMI-HUMANOID ROBOT POSTURE WITH RESPECT TO EXTERNAL DISTURBANCES\***

*UDC 004.896:61 681.532.1*

**Vesna Antoska<sup>1</sup>, Veljko Potkonjak<sup>2</sup>,  
Mile J. Stankovski<sup>3</sup>, Nenad Baščarević<sup>2</sup>**

<sup>1</sup>Faculty of Technology and Technical Science,  
Ss. Climent Ohridski University – Bitola, Republic of Macedonia  
<sup>2</sup>Faculty of Electrical Engineering, University of Belgrade, Serbia  
<sup>3</sup>Faculty of Electrical Engineering and Information Technology  
Ss. Cyril and Methodius University – Skopje, Macedonia

**Abstract.** This paper applies sophisticated methods developed for mathematical modeling of semi humanoid robot (driven robot) to real motions, particularly in posture stabilization for different situation. A general simulation system is realized: following deductive principle, i.e. to start from a completely general model applicable to a set of tasks. Such a model is further adjusted according to need certain specific situations. Simulation is applied to a problem which is important for semi-humanoid robot, namely the stabilization of posture being subject to different disturbances. To ensure stability of the robot position, the robust control is evaluated. Simulations are carried out and the influence of different cart movements on the robot balance is analyzed by comparing different cases.

**Key words:** *Semi-Humanoid Robot, Robot, Robustness, Robot Posture*

### **1 . INTRODUCTION**

This work considers a new and generalized approach to the modeling of human and humanoid motion. In principle, modeling may follow an *inductive* approach or a *deductive* one. We use the term *flier*. This situation is not uncommon in reality. However, such motions are still less common than those where the system is in contact with the *ground* or some other supporting *object* in its environment.

---

Received December 10, 2012

**Corresponding author:** Vesna Antoska

Faculty of Technology and Technical Science, Ss. Climent Ohridski University – Bitola, Republic of Macedonia  
E-mail: vesna.antoska@uklo.edu.mk

\* **Acknowledgments:** This work is part of EU 2007-2013 - Challenge 2- Cognitive Systems, Interaction, Robotics - under grant agreement no. 231864 - ECCEROBOT; and partly by the Serbian Ministry of Science and Technological Development under contract 35003 and 44008. ECCEROBOT- "Embodied Cognition in a Compliantly Engineered Robot" ([www.eccerobot.org](http://www.eccerobot.org))..

The concept of the *flier* approach, derived for humanoid robots, is then applied [3,4]. It originally dealt with a full humanoid (pelvis, torso, arms, legs, and head). ECCEROBOT applies only a part of it to the upper-body robot of Fig. 1. In the past few years a new expression has been established –anthropomimetic [2].

Anthropomimetics refers to a new kind of robotics which copies the human body as faithfully as possible with the aim of achieving the level of performances (diversity of motions, manoeuvrability, etc.) comparable with that of a human.

ECCEROBOT has joints driven by antagonistically coupled DC motors. The two joint motors, the agonist and antagonist, working through tendons, mimic muscles. It pertains to a new class of principle in robot construction, which tries to copy the human body (configuration) as faithfully as possible. The goal is not just to replicate human structure, but also to attain a high level of performances (diversity of motions, manoeuvrability, etc.) analogous to human abilities. This paper has a more concrete focus – it examines the problem of posture and its robustness to external disturbances. So this paper attempts to establish the cart dimensions to obviate overturning and to find the constraints in motion capabilities of the wheeled robot that is presented by the model for an existing anthropomorphic humanoid – ECCEROBOT<sup>1</sup>.

The usual approach to the analysis of dynamic balance is based on ZMP theory originally developed to control human-or-humanoid walk [7-9].

## 2. SYSTEM CONFIGURATION

The ECCEROBOT project is attempting to create a robot very similar in function to the human body, by replicating its skeleton and its antagonistic tendon drives. With its compliant human-like shape, such a mechanism is able to interact with humans and with its environment in an inherently safe way. Instead of just copying the outward form of a human, it copies the inner structures and mechanisms – bones, joints, muscles, and tendons – and thus has the potential for human-like action and interaction in the world. ECCEROBOTs skeleton is a very detailed replicate of the human model, consisting of bones and joints formed out of polymorph (new type of thermoplastics which has bone like appearance when it is cold).

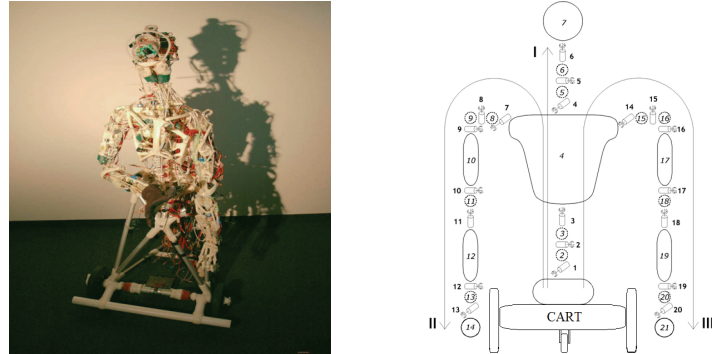


**Fig. 1.** (a) ECCEROBOT placed on the three wheel base (b) The robot model structure

<sup>1</sup> EU FP7 project: „Embodied Cognition in a Compliantly Engineered Robot“ ([www.eccerobot.org](http://www.eccerobot.org))

ECCEROBOT joints are driven by the two antagonistically coupled artificial muscles similar to the most of the human muscles responsible for movements, instead of high precision actuators and stiff components as in typical humanoid robots. These muscles are introduced as the combination of non-elastic threads, elastic tendons and DC motors equipped with gear-boxes. Thus, desirable mechanical compliance is achieved by using elastic spring for connecting non-elastic thread to the robot links, copying human muscle and tendon. Following the anthropomimetic principle [2], ECCEROBOT is aimed to be the first one with a great dose of self consciousness.

The joints presented in Fig. 1 are actuated by two DC motors working in an antagonistic mode. All joint models do not have the same structure. They are divided in two groups:

- ‘triangular’ model – used for the elbow rotation, motor ‘a’ imitates the role of the biceps (or brachialis) while motor ‘b’ mimics the triceps (mechanical model is shown in Fig. 2)
- ‘circular’ model – used for the shoulder, waist, neck and wrist rotation (mechanical model is shown in Fig. 2)

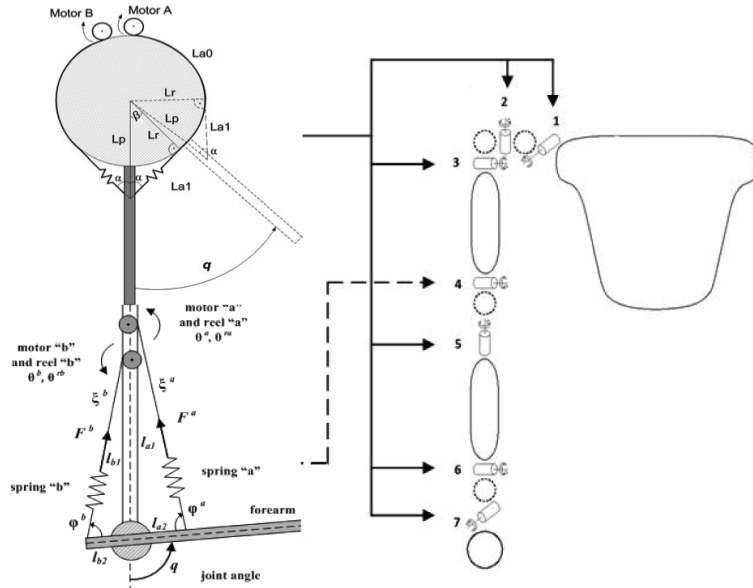


**Fig. 2.** Elbow rotation with AA drives – triangular model  
Shoulder rotation AA drives - circular model

The full dynamic modeling of the complete body mechanism integrated with the presented joint-drive models is elaborated in [16]. The model (1)–(4) is derived considering contacts dynamics as well, as an essential part of the humanoid working in presence of humans. It is based on the intensive research on humanoid dynamics and modeling of the humanoid robots presented in [17, 18]. In the current project legs are replaced by a wheeled base (the cart), see Fig. 2. The cart is used to perform the global motion i.e. take the robot to the place where some work is to be done.

### 3. MATHEMATICS

We start from the ‘classical’ dynamic model that considers the joint torques as the controls and relates them to joint motions. The concept of the Flier approach, derived for humanoid robots [17,18]. It originally dealt with a full humanoid (pelvis, torso, arms, legs, and head). ECCEROBOT applies only a part of it to the upper-body robot. The system configuration becomes as shown in Fig. 3.

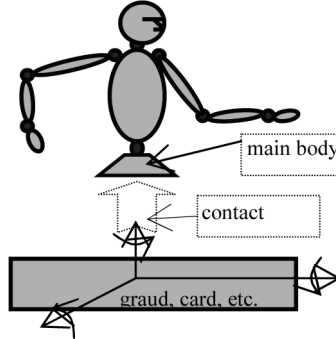


**Fig. 3.** The system configuration

The idea of the *flier* approach is to consider the humanoid freely flying in space and then to introduce contacts with environmental objects in order to model the imposed motion task. This applies to any motion task: walking and running, manipulation, sporting motions, etc. When applied to the ECCEROBOT structure (Fig. 1.b).

Following the flier concept, we start the dynamic analysis from the free-flying model. If robot has  $n$  single-rotation joints ( $n = 20$  for the configuration under investigation), then its position is defined by a vector of dimension  $N = 6 + n$ :

$$\begin{aligned} Q_{N \times 1} &= [X \quad q]^T = [x \quad y \quad z \quad \theta \quad \varphi \quad \psi \quad q_1 \quad q_2 \quad q_3 \quad \dots \quad q_n]^T \\ Q_{N \times 1} &= (X_{6 \times 1}, \quad q_{6 \times 1}) \end{aligned} \quad (1)$$

where  $X = (x, y, z, \theta, \varphi, \psi)$  defines the absolute position of the ‘main body’, the pelvis in this case, while  $q = (q_1, \dots, q_n)$  represents joint angles.

The dynamic model has the matrix form:

$$H(Q)\ddot{Q} + h(Q, \dot{Q}) = T \quad (2)$$

where  $T_{N \times 1} = (0, \dots, 0, \tau_1, \dots, \tau_n) = (0_{6 \times 1}, \tau_{n \times 1})$  is the generalized vector of drives,  $\tau = (\tau_1, \dots, \tau_n)$  represents the joint torques,  $H_{N \times N}$  is the inertial matrix, and  $h_{N \times 1}$  takes care of gravity, centrifugal, and Coriolis’ effects.

The contacts (one or more) with the environment are now introduced. Contact refers to a particular robot link and restricts the relative motion of that link with respect to the relevant environmental object. If there are  $m$  restricted directions, the contact can be expressed as:

$$\dot{s}^c(Q, Q_b) = 0 \quad (3)$$

where  $s^c_{mix}$  is the vector of relative link-to-object position, which depends on the robot position  $\mathbf{Q}$  (of dimension  $N$ ) and the object position  $\mathbf{Q}_b$  (of dimension  $k$ ). By derivation:

$$\begin{aligned} \dot{s}^c &= J(Q, Q_b) \dot{Q} + J_b(Q, Q_b) \dot{Q}_b = 0 \\ \ddot{s}^c &= J(Q, Q_b) \ddot{Q} + J_b(Q, Q_b) \ddot{Q}_b + A(Q, \dot{Q}, Q_b, \dot{Q}_b) = 0 \end{aligned} \quad (4)$$

where  $J = \partial s^c / \partial Q$  and  $J_b = \partial s^c / \partial Q_b$  are Jacobians of dimensions  $m \times N$  and  $m \times k$  respectively, and  $A$  contains second partial derivatives.

Contact introduces reaction forces and moments. Reactions appear along the restricted directions  $\mathbf{s}_c$ . Let  $\mathbf{R}_{mx1}$  be the vector of reactions.

The dynamics of the contact motion is now described by the model:

$$H(Q) \ddot{Q} + h(Q, \dot{Q}) = T + J^T(Q, Q_b) R \quad (5a)$$

$$\ddot{s}^c = J(Q, Q_b) \ddot{Q} + J_b(Q, Q_b) \ddot{Q}_b + A(Q, \dot{Q}, Q_b, \dot{Q}_b) = 0 \quad (5b)$$

$$W(Q_b) \ddot{Q}_b + w(Q_b, \dot{Q}_b) = T_b - J_b^T(Q, Q_b) R \quad (5c)$$

$$\bar{H} \ddot{\theta} + \bar{h}(Q, \dot{Q}, \theta^a, \dot{\theta}^a, \theta^b, \dot{\theta}^b) = C u \quad (5d)$$

The model (5) contains the robot dynamics ( $N$ -dimensional submodel (5a)), the object dynamics ( $k$ -dimensional submodel (5c) with model matrices  $\mathbf{W}_{k \times k}$  and  $\mathbf{w}_{k \times 1}$ ), and the geometry of contact ( $m$ -dimensional subsystem (5b)). Equation (5d) describes dynamics of the antagonistically coupled drives including motors and gearboxes. It relates the control inputs ( $\mathbf{u}_{2m \times 1}$  antagonistic motors voltages for the robot and  $T_b$  driving torque for the object) to the motion ( $R_{N \times 1}$ ,  $\theta_{2n \times 1}$  and  $Q^b_{k \times 1}$  for the robot, antagonistically coupled motors and the object respectively) and the contact reactions ( $R_{k \times 1}$ ). The matrices  $H$ ,  $h$ ,  $W$ ,  $w$ ,  $\bar{H}$ , and  $\bar{h}$ , are robot's inertial matrix; matrix that takes care of gravity, centrifugal, Coriolis' effects, and joint geometry; inertial matrix of the object; similar effects referring to object; two matrices describing dynamics of the antagonistically coupled drives respectively. The vector  $s^c$  represents constrained coordinates due to in contact motion, while the  $J$ ,  $J_b$ , and  $A$ , are appropriate Jacobians and adjoined matrix.

If we consider motion of the contacted object (in this case mobile wheeled base) as prescribed –  $Q_b$ , the object dynamics is omitted and model becomes:

$$H(Q) \ddot{Q} + \tilde{h}(Q, \dot{Q}, \theta^a, \dot{\theta}^a, \theta^b, \dot{\theta}^b) = J^T(Q, Q_b) R \quad (6a)$$

$$\ddot{s}^c = J(Q, Q_b) \ddot{Q} + J_b(Q, Q_b) \ddot{Q}_b + A(Q, \dot{Q}, Q_b, \dot{Q}_b) = 0 \quad (6b)$$

$$\bar{H} \ddot{\theta} + \bar{h}(Q, \dot{Q}, \theta^a, \dot{\theta}^a, \theta^b, \dot{\theta}^b) = C u \quad (6c)$$

The model (5) enables integration of the system and therefore simulation of the anthropomorphic robot on the mobile base. This means that for given control voltages  $\mathbf{u}$  and knowing object motion  $Q_b$  one can calculate robot motion  $Q$ , motor positions  $\theta$  and reaction forces/torques  $R$ .

Therefore, the target configuration of the anthropomorphic robot moving on the three wheeled mobile base is tested in Section 5, and examination of the cart design and movement limits are carried out using derived model.

#### 4. CONTROL ISSUE

In this Section a brief overview of the control strategy used for controlling the ECCEROBOT concept is presented. The control algorithm based on a biologically inspired and energy efficient approach – *the puller-follower concept* [19], which distinguishes between and separates the roles of the agonist and antagonist motors. The main issue of the system, based on the biological similarity to human beings, is the control of the antagonistically coupled electrical drives in order to achieve desired joint position. This action requires that the motors should be driven simultaneously, in a coordinated way. One motor, *the puller*, takes the main responsibility for this task. In order to prevent slackening of the antagonist tendon, a second control task – maintaining an appropriate tension in the tendon – is added. This additional task is mainly assigned to *the follower* motor. The joint motors exchange roles when the motion requires it, usually when acceleration turns to deceleration. This exchange of roles is called *switching*. It is important to point out that antagonistic motor always have opposite roles. The solution we propose for this problem in multi-jointed system is a robust control design [20], together with nonlinear compensation for the effects of gravity, uncertain effective joint inertia and dynamic coupling between joints. Having secondary importance for this paper just the basic idea and outline of the control concept is given.

#### 5. SIMULATION RESULTS

The aim of the simulation analysis is checking to what extent the ECCEROBOT can stand the disturbance resulting from different cart movements and finding the cart dimensions which disable overturning of the robot during some common tasks. As it is expected, the robot can easily handle low speed cart movements, and intuitively problems appear with increase in speed. We restricted the consideration to cart motions which are relevant to the humanoid robot working in human centred environment. Namely, a mobile robot is usually intended to work in services – so in homes, department stores, restaurants, museums, hospitals, etc.

The selection of the robot drives is essential for the simulation results and therefore for establishing the limits of the robot acting. The ECCEROBOT uses Maxon products, and for this study following motor and gearboxes are chosen:

- Waist joints use 148877 DC motor RE40 48V and 203116 Gearbox GP42C 15:1
- Shoulder joints use 268193 DC motor RE30 12V and 326664 Gearbox GP32HP 51:1
- Neck, elbow and wrist joints use 118637 DC motor RE13 12v and 110315 Gearbox GP13A 67:1

#### A. ZMP Criterion

The ZMP calculation is used to identify the robot stability. The term and solid mathematical background of the ZMP method are presented in the pioneer work of its authors Vukobratovic and Stepanenko [21], and later by his associates [11]. The main contribution of the ZMP criterion claims that if the ZMP is inside the boundaries of support polygon, then the robot is able to keep the balance. The support polygon presenting desir-

able/stable region is determined by the feet shape and position in a case of legged robot or by the wheel position in a case of mobile robot with wheels. An equilateral triangle (sides are denoted as  $a$ ) formed by the three wheel assemblies represents the support polygon and therefore the stable region for our case of ECCEROBOT standing on the three wheeled mobile base (see Fig. 5). For simplicity, we suppose the three wheels are disseminated equally. Although, the stable region is sufficient to prevent the robot from falling over, we introduce the valid stable region (circle inscribed in the triangle of the stable region with radius  $r$ ) in order to simplify our calculations for the platform dimensions. Furthermore, this area demands stronger restriction than equilateral triangle and gives the reasonable stability margin. The most stable point on the platform is the centre of the inscribed circle.

Quite similar approach is proposed in [13]. In our case this method is utilized with a slight difference, assuming that we are not totally restricted to an existing mobile platform. We have the cart construction, but the appropriate cart dimensions which ensure the robot stability have to be determined. Therefore, some conditions are different from those in [13].

The area of the valid stable region (shown in Fig. 5) is defined by

$$S : x_{zmp}^2 + y_{zmp}^2 \leq r^2 \quad (7)$$

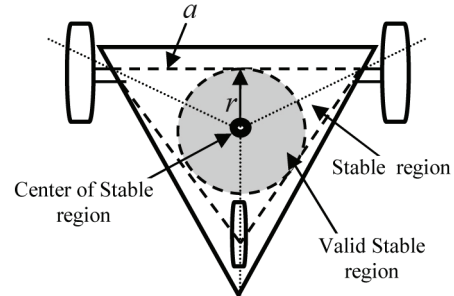
where  $x_{zmp}$ ,  $y_{zmp}$  denote  $x$  and  $y$  coordinates of ZMP,  $S$  and  $r$  represents the valid stable region and its radius, respectively. If the ZMP coordinates go out of the stable region, then the robot starts overturning.

The cart is driven in a ‘classical’ way: there are no tendons or antagonistic actions; there is one standard bidirectional DC motor per wheel (currently, front wheels are actuated). Transmission involves gearing. Therefore, there is no compliance between the motor and the wheel shaft. In such case, sufficiently strong motors and sufficiently strong PID control turned out as just enough to provide high-quality tracking regardless of the robot behaviour. Therefore, a disturbance coming from the robot movements can be easily overcome, and therefore cart dynamics can be omitted and cart motion can be used as prescribed. So, just the cart kinematics is considered for the analysis of the robot balance and further analysis.

During these cart movements the robot has a task to keep the prescribed position (up-right torso position with bent elbows for  $15^\circ$  and outstretched forward arms for  $30^\circ$ ).

The typical cart movements are examined:

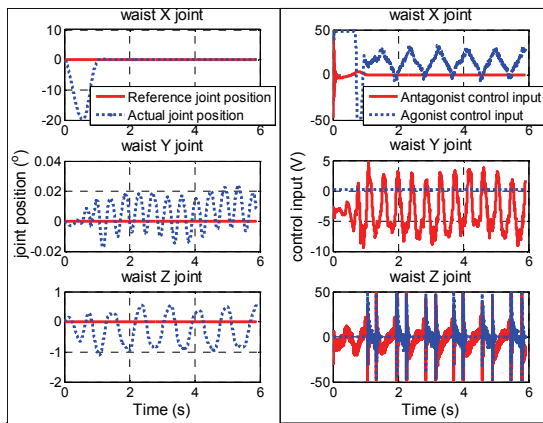
- **Linear (longitudinal) and lateral acceleration** – there are three phases in this motion: acceleration and deceleration take 40% of the total task time (equally divided, 20%+20%) and the rest of the time (60%) the cart moves with constant velocity. So, this is trapezoidal velocity profile.



**Fig. 5.** The Sketch map of the cart assemblies (bird's-eye view)

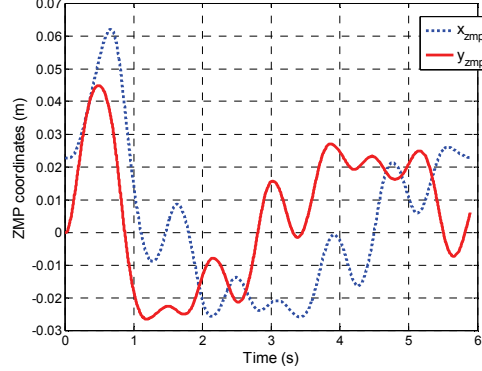
- **Oscillations in longitudinal direction (forward-backward)** – this is a sine wave motion; one full time period is taken for testing, so the starting and the terminal positions are identical.
- **Gyre (circular motion)** – emulates the situation when the cart moves along a winding road (alternation of left and right curves): the intention is to test the centrifugal lateral effects. The path is one full circle.
- **Oscillations of the yaw angle** – this is the way to describe the twisting motion. It reveals the influence of the change in cart direction (i.e. the influence of the cart angular acceleration) to the robot behavior. Sine function is used to emulate a twisting motion. One full time period is taken for testing.
- **Pitch and roll angle** - if driving a cart along a waved road (truly bumpy road is not expected), the lateral and the longitudinal axes move up and down. This is described by the oscillatory roll and pitch angle, respectively. Sine function is used to emulate a road causing the pitch and roll inclination. One full time period is taken for testing.

Fig. 5 shows the time histories of robot waist joint positions as crucial for keeping the balance, and its control signals during the circular movement (radius 3m and time period 5.9s). The number of shown joints is reduced to three (the robot has 20 joints). The stability of the robot depends on the stability of the waist joints; hence, the results for these joints have to be shown. The behaviour of other joints has also an effect on the stability, but much less than the three waist joints. The strongest influence is on the waist X joint, as we expected. The centrifugal force acts along axis  $y$ , so the waist X joint endures most of the disturbance. This effect is followed by the max voltage of the control input as long as the position deviation is not reduced. Further increase of the acceleration magnitude (reducing the time period) would increase the deviation in the waist X joint, leading to the robot tipping-over. This fact is the consequence that the control signal cannot increase the voltage above its max value (48V) and that is not sufficient to withstand larger disturbance caused by centrifugal effect. In this manner the control limits are reached and they cannot be improved.



**Fig. 6.** Position and control inputs of the waist joints during the cart circular motion – radius 3m, time period 5.9s

ZMP coordinates during this motion are presented in Fig. 7. At the beginning the deviation is the most emphasized, which is the result of the waist X joint behaviour during that period.



**Fig. 7.** ZMP coordinates of the waist joints during the cart circular motion – radius 3m, time period 5.9s

The cart dimensions have to withstand the max variation (from its initial position) of the ZMP coordinates, otherwise the robot will tip-over. Based on this statement, the fitting wheel dimensions have to be calculated in order to prevent the robot from falling over. To solve this problem we use (7) to obtain the radius of the valid stable region S. Relying on radius and characteristics of the equilateral triangle, we can easily calculate side  $a$ , which is the min value of the cart dimension and ensures the robot to keep its balance.

**Table 1.** Characteristics of the cart roll, pitch and yaw oscillations

	Roll		Pitch		Yaw	
Amplitude (deg)	20	30	20	30	45	60
Time (s)	1.85	2.3	1.8	2.35	1	1.1
max Acceleration (deg/s <sup>2</sup> )	229	224	244	214	1776	1960
max Velocity (deg/s)	68	82	70	80	282	343
max $x_{zmp}$ (cm)	0	0.1	11.8	17.4	2.8	3.9
max $y_{zmp}$ (cm)	16	18.3	0	0	3.6	3.5
Cart dim. $a$ (cm)	55.5	63.4	40.9	60.3	15.8	18.2

**Table 2.** Characteristics of the cart circular and forward - backward motions

	Gyre			Forward-Backward		
Radius/Amplitude (m)	1	2	3	1	2	3
Time (s)	3.4	4.8	5.9	2.4	3.15	3.7
max Acceleration (m/s <sup>2</sup> )	6.83	6.81	6.85	6.9	7.95	8.65
max Velocity (m/s)	1.85	2.62	3.2	2.6	4	5.1
max $x_{zmp}$ (cm)	7.5	7	3.9	5.2	4.1	9.2
max $y_{zmp}$ (cm)	3.2	4.8	4.5	0	0	0
Cart dim. $a$ (cm)	28.3	29.4	20.7	18	14.2	31.9

**Table 3.** Characteristics of the cart longitudinal and lateral motions

	Longitudinal trapez.	Lateral trapez.
Distance (m)	10	10
Time (s)	4.5	4.75
Acceleration ( $m/s^2$ )	3.1	2.75
max Velocity ( $m/s$ )	2.79	2.61
max $x_{zmp}$ (cm)	9.6	0.1
max $y_{zmp}$ (cm)	0.7	6.3
Cart dim. $a$ (cm)	33.4	21.8

If side  $a$  is enlarged, it would not provide increasing of the cart max velocity and max acceleration because we reached the control limits and that cannot be ameliorated. Finding the wheel dimensions prevents from overturning caused by changeable ZMP and it just enables to exploit the control to the maximum. Previously said can be applied to circular motion presented in Figs. 6-7. Max deviations of the ZMP coordinates are  $x_{zmp} = 3.9\text{cm}$  and  $y_{zmp} = 4.5\text{cm}$ . Now we use (7) to obtain radius  $r = 5.95\text{cm}$ . Connection between radius of the inscribed circle and sides of equilateral triangle is  $a = 6r / \sqrt{3}$ , so in our case  $a = 20.63\text{ cm}$ . The main characteristics of all examined cart movements are shown in Tables 1-3. Some reasonable values (for our needs) of amplitudes and distances are taken into consideration.

Relying on the evaluated results from Tables 1-3, the max value of cart dimension  $a$  is 63.4cm. With this result, tip-over stability for all examined cart motions is ensured.

We should point out one more thing. Satisfactory results for max velocities and accelerations for all movements are obtained. Giving an example for longitudinal motion with trapezoidal velocity profile, the max velocity is  $2.79\text{ m/s}^2$  (approximately around  $10\text{ km/h}$ ). This is a very good achievement, having in mind that the most advanced bipedal robot Honda's ASIMO provides max speed of  $9\text{ km/h}$  in ideal conditions.

## 6. CONCLUSION

Finding the boundaries of the proposed control algorithm and establishing the cart dimensions to avoid the mobile robot (during different cart motions) from tipping-over was the topic of this research. Bearing in mind that the robot has compliant actuation (expandable tendons) makes it more sensitive to external influence. Any disturbance can cause oscillation accompanied with a specific and potentially highly risky situation – the resonance. The cart motion (acceleration or deceleration, turning left or right, moving up-hill/downhill, rolling, etc.) strongly influences the robot behaviour. Therefore, robust robot control was absolutely necessary to enable examination of the complete anthropomorphic robot behaviour on the mobile base, and check its behaviour in such disturbances. Our experiments have demonstrated that tip-over stability of the robot can be preserved for some ‘reasonably’ fast movements of the cart, relying on the appropriate cart design. The cart design has been proposed by robot balance analysis through the ZMP criterion. The obtained results are encouraging and it proves that a compliant anthropomorphic mobile

robot could be used to work in services - in homes, department stores, restaurants, museums, hospitals, etc., despite of its very complex structure and demanding control requirements.

Since adding legs would still be a very challenging task, the future work would consider the cart testing in some realistic situation involving friction, slip and contact forces between the wheels and the ground. Further research can explore the method for cart design as more general, and not only be restricted to equilateral triangle (depends on the cart shape).

## REFERENCES

1. Y. Sakagami, R. Watanabe, C. Aoyama, S. Matsunaga, N. Higaki, and K. Fujimura, "The intelligent ASIMO: system overview and integration", *In Proc. of International Conference on Intelligent Robots and Systems (IROS 2002)*, Lausanne, Switzerland, 2002, pp. 2478–2483.
2. O. Holland, and R. Knight, "The Anthropomimetic Principle", *In Proc. of the Symposium on Biologically Inspired Robotics* edited by J. Burn and M. Wilson (AISB06), Bristol, UK, 2006
3. R. Holmberg, and O. Khatib, "Development and Control of a Holonomic Mobile Robot for Mobile Manipulation Tasks", *International Journal of Robotics Research*, vol. 19, no. 11, 2000, pp. 1066–1074.
4. K. Sreenath, H. W. Park, I. Pouliquen, and J. Grizzle, "A Compliant Hybrid Zero Dynamics Controller for Stable, Efficient and Fast Bipedal Walking on MABEL", *The International Journal of Robotics Research*, vol. 30, no. 9, 2011, pp. 1170–1193.
5. Y. Fukuoka, H. Kimura, and A. Cohen, "Adaptive Dynamic Walking of a Quadruped Robot on Irregular Terrain Based on Biological Concepts", *The International Journal of Robotics Research*, vol. 22, no. 3-4, 2003, pp. 187–202.
6. J. Wang, and Y. Li, "Kinematics and Tip-over Stability Analysis for a Mobile Humanoid Robot Moving on a Slope", *IEEE International Conference on Automation and Logistics*, Qingdao, China, 2008, pp. 2426–2431.
7. J. Wang, and Y. Li, "Static Force Analysis for a Mobile Humanoid Robot Moving on a Slope", *IEEE International Conference on Robotics and Biomimetics (ROBIO08)*, Bangkok, Thailand, 2009, pp. 371–376.
8. J. Wang, Y. Li, and C. Qiu, "Analysis of Dynamic Stability Constraints for a Mobile Humanoid Robot", *IEEE International Conference on Robotics and Biomimetics (ROBIO08)*, Bangkok, Thailand, 2009, pp. 639–644.
9. M. Stilman, J. Wang, K. Teeyapan, and R. Marceau, "Optimized Control Strategies for Wheeled Humanoids and Mobile Manipulators", *IEEE International Conference on Humanoid Robots*, Paris, France, 2009, pp. 568–573.
10. B. Thibodeau, P. Deegan, and R. Grupen, "Static Analysis of Contact Forces With a Mobile Manipulator", *In Proc. of the 2006 IEEE International Conference on Robotics and Automation*, Orlando, USA, 2006, pp. 4007–4012.
11. M. Vukobratovic, and B. Borovac, "Zero-Moment Point — Thirty Five Years of its Life", *International Journal of Humanoid Robotics*, vol. 1, no. 1, 2004, pp. 157–173.
12. S. Sugano, Q. Huang, and I. Kato, "Stability Criteria in Controlling Mobile Robotic Systems", *In Proc. of the 1993 IEEE/RSJ International Conference on Intelligent Robots and Systems*, Yokohama, Japan, vol. 2, 1993, pp. 832–838.
13. Y. Li, D. Tan, Z. Wu, and H. Zhong, "Dynamic Stability Analyses Based on ZMP of a Wheel-based Humanoid Robot", *In Proc. of the 2006 IEEE International Conference on Robotics and Biomimetics*, Kunming, China, 2006, pp. 1565–1570.
14. J. Kim, and W. Chung, "Real-time ZMP Compensation Method using Null Motion for Mobile Manipulators", *Proceedings of the 2002 IEEE International Conference on Robotics & Automation*, Washington, DC, USA, vol. 2, 2002, pp. 1967–1972.
15. V. Potkonjak, B. Svetozarevic, K. Jovanovic, and O. Holland, "Biologically-inspired Control of a Compliant Anthropomimetic Robot", *The 15th IASTED International Conference on Robotics and Applications*, Cambridge, Massachusetts, 2010, pp. 182–189.
16. V. Potkonjak, K. Jovanovic, B. Svetozarevic, O. Holland, and D. Mikicic, "Modelling and Control of a Compliantly Engineered Anthropomimetic Robot in Contact Tasks", *In Proc. of Mechanisms and Robotics Conference (ASME2011)*, Washington, DC, USA, 2011, in press.
17. V. Potkonjak, and M. Vukobratovic, "A Generalized Approach to Modeling Dynamics of Human and Humanoid Motion", *International Journal of Humanoid Robotics*, vol. 2, no. 1, 2005, pp. 1–24.

18. V. Potkonjak, M. Vukobratovic, K. Babkovic, and B. Borovac, "Simulation Model of General Human and Humanoid Motion," *Multibody System Dynamics*, vol. 17, no. 1, 2007, pp. 71-96.
19. V. Potkonjak, B. Svetozarevic, K. Jovanovic, and O. Holland, "Control of Compliant Anthropomorphic Robot Joint", In Proc. of International Conference of Numerical Analysis and Applied Mathematics (ICNAAM 2010), Rhodes, Greece, 2010, pp. 1271-1274.
20. V. Potkonjak, K. Jovanovic, P. Milosavljevic, N. Bascarevic, and O. Holland, "The Puller-Follower Control Concept For The Multi-Joint Robot With Antagonistically Coupled Compliant Drives", In Proc. of IASTED International Conference on Robotics (ROBO2011), Pittsburgh, USA, 2011, pp. 375-381.
21. M. Vukobratovic, A. Frank, and D. Juricic, "On the stability of biped locomotion", *IEEE Transaction on Biomedical Engineering*, vol. 17, 1970, pp. 25-36.

## ROBUSNOST POLU-HUMANOIDNOG POLOŽAJA ROBOTA U ODNOSU NA SPOLJAŠNJE POREMEĆAJE

**Vesna Antoska, Veljko Potkonjak,  
Mile J. Stankovski, Nenad Baščarević**

*Ovaj rad prikazuje primenu sofisticiranih metoda razvijenih za matematičko modelovanje polu humanoidnih robota za realne pokrete, naročito u stabilizaciji držanja u različitim situacijama. Ostvaren je opšti simulacioni sistem: prati se deduktivni pristup, to jest, počinje se od potpuno opšteg modela primenljivog na set zadataka. Takav model se dalje usklađuje prema zahtevima određene specifične situacije. Simulacija se primenjuje na problem koji je važan za polu humanoidne robe, a to je pitanje držanja na koje utiču različiti uticaji. Da bi se osigurala stabilnost pozicije robota, procenjuje se kontrola robustnosti. Izvode se simulacije i analizira se uticaj različitih pokreta na balans robota poredanjem različitih situacija.*

Ključne reči: *polu-humanoidni robot, robot, robustnost, položaj robota*